The Effect of Ferrous Iron on Mineral Scaling During Oil Recovery

Torstein Haarberg,* Jens E. Jakobsen and Terje Østvold†

Institute for Inorganic Chemistry, Norwegian Institute of Technology, N-7034 Trondheim, Norway

Haarberg, T., Jakobsen, J. E. and Østvold, T., 1990. The Effect of Ferrous Iron on Mineral Scaling During Oil Recovery. – Acta Chem. Scand. 44: 907–915.

A model for the solubility, K_{sp}, of $FeCO_3$ based on Pitzer's equation for activities in aqueous electrolyte is presented. The model predicts the solubility of $FeCO_3$ with varying composition in the system

H_2O–OH^-–H^+–CO_2–HCO_3^-–CO_3^{2-}–SO_4^{2-}
–Cl^-–A^-–Na^+–K^+–Fe^{2+}–Mg^{2+}–Ca^{2+}–Sr^{2+}–Ba^{2+}

in the temperature and pressure regions: $0 < T < 200\,°C$, $0 < P_{CO_2} < 300$ bar, $P_{tot} < 1000$ bar. A comparison between model calculations and available experimental data gives a relative standard deviation, $SD_{rel} < 10\,\%$.

Model solubilities of all the scaling minerals together with the new model for the solubility of $FeCO_3$ are used in an equilibrium approach to calculate how mineral precipitation during oil recovery may depend on Fe^{2+} ion concentrations in produced waters. $FeCO_3$ precipitation from water containing as much as 100 ppm Fe^{2+} results in decreasing $CaCO_3$ precipitation, leaving the total carbonate precipitation approximately constant as long as the calcium concentration is much larger than the iron concentration. This is normally the case in sea and formation waters. When acetic acid is introduced into the water keeping the total alkalinity constant, $CaCO_3$ precipitation is reduced while $FeCO_3$ precipitation is constant up to the $CaCO_3$ solubility limit. At higher concentrations of acid, $FeCO_3$ precipitation is reduced as expected.

During oil recovery mineral precipitation may occur from the produced waters. This precipitation may lead to well damage, closing of production tubing and malfunctioning of production equipment, resulting in heavy production losses and expensive clean-up operations. To remedy this situation the oil companies have to treat their wells with scale inhibitors when the produced waters indicate possible mineral precipitation. It is therefore necessary to have models which give reliable mineral precipitation predictions. Many such models are in use today. The weaknesses with many of these models are usually: (i) the effect of pressure on solubility is not considered, (ii) the activity coefficient corrections are not based on proper thermodynamic models, and (iii) reaction kinetics of the precipitating reactions are not considered.

To remedy this situation Haarberg and co-workers [1–4] introduced a model in which all the abovementioned factors were considered. In their model Haarberg and co-workers used an algorithm which could either model the equilibrium in the multicomponent system[1,2] or also take into consideration the kinetics of the precipitation reactions.[3] It is of vital importance to include the kinetics of these reactions in a prediction of the build-up of scale in those areas of the production system where liquid flow rates are high. Such areas are the near-well area and the procution tubing and equipment.

From thermodynamic solubility products, $K°_{sp}$, which can easily be obtained from experimental data in pure H_2O–MX systems for which the MX solubility is very small, Haarberg and co-workers[1,2,4] calculated the solubilities of the scale formers at high ionic strength using proper activity coefficients. In their first approach[1,2] the UNIQUAC[5] model was combined with the Debye–Hückel and Brønsted–Guggenheim models. This model, however, does not properly describe ionic interactions, and may fail to predict activity coefficients with reasonable accuracy at high ionic strength in special cases. We have therefore in the latest version of our model[3,4] substituted the UNIQUAC activities by activities based on a model developed by Pitzer.[6–8] In the present paper the Pitzer model is used to obtain activity coefficients for Fe^{2+} and other aqueous species at varying concentrations and temperatures.

The concentration of naturally dissolved iron in formation waters encountered in oil and gas production is normally around 10 ppm, and is rarely more than 100 ppm.[9] Corrosion during production and acidification of wells may, however, easily lead to a multifold increase in the concentration of iron.

The more common forms of iron scale are rust (different types of iron oxides), iron sulfides [pyrite (FeS_2), kansite (Fe_9S_8) and pyrrhotite ($F_{0.875}S$)] and the iron carbonate scales siderite ($FeCO_3$) and siderite containing Mn and Mg ions.

In the present paper we will deal only with the additional scale problem arising from $FeCO_3$ precipitation.

If H_2S is present in the water, the pH and thus the

* Present address: Hydro Aluminium, Årdal Verk, N-5875 Årdalstangen, Norway.

† To whom correspondence should be addressed.

equilibria in the carbonate system will be changed. The presence of both H_2S and Fe^{2+} in the water may cause precipitation of FeS. FeS scaling will be dealt with in a forthcoming paper.

The solubility model for $FeCO_3$

Experimental data for the pressure dependence of the solubility product of $FeCO_3$ are not available. This quantity may, however, be calculated using eqn. (1),[2] where ΔV and

$$\left(\frac{\mathrm{d}\ln K_{sp}}{\mathrm{d}P}\right)_T = -\Delta V/RT + \Delta KP/RT \qquad (1)$$

ΔK are the changes in volume and compressibility for the dissolution reaction of $FeCO_3$(s) in water. $\Delta V°_{25\,°C} = -58.9$ cm^3 mol^{-1} for $FeCO_3$(s) dissolution,[10] while data at higher temperatures are not available. For $CaCO_3$ $\Delta V°_{25\,°C} = -58.54$ cm^3 mol^{-1} for the equivalent reaction.[11] Compressibility data for Fe^{2+} are not available. Owing to the equal $\Delta V°_{25\,°C}$ data for $FeCO_3$ and $CaCO_3$ and to the lack of volume data for $FeCO_3$(aq) at higher temperature and pressure, we have therefore assumed that the pressure dependences of the $FeCO_3$ and $CaCO_3$ solubility products are equal. In Table 1 the values of ΔV and ΔK in pure water used in eqn. (1) in the temperature region $25 \le T \le 150$ °C are given.

To calculate the solubility of $FeCO_3$ in aqueous solutions, however, we also have to take into consideration that the concentration of CO_3^{2-} may change with pressure owing to the pressure dependence of the carbonate equilibria (2)–(4). The reaction volumes for eqns. (2)–(4) are, however,

$$CO_2\,(g) = CO_2\,(aq) \qquad (2)$$

$$H_2O + CO_2\,(g) = HCO_3^- + H^+ \qquad (3)$$

$$HCO_3^- = CO_3^{2-} + H^+ \qquad (4)$$

not well known.[2] Experimental data indicate $\Delta V°$[eqn. (3)] $\approx \Delta V°$[eqn. (4)].[2] As a first approximation we have assumed that the ΔV values for eqns. (2)–(4) are independent of concentration. Since this assumption obviously is rather rough, and since the compressibility changes for the same reactions only give a minor correction to the pressure dependence of the equilibrium constants, we have neglected the pressure effect on the reaction volumes of eqns. (2)–(4). The ΔK value used in eqn. (1) is furthermore assumed to be independent of both temperature and composition.

Table 1. ΔV as obtained by Haarberg[12] and ΔK as given by Millero[11] for the reaction $CaCO_3$(s) = $CaCO_3$(aq) in pure water.

T/°C	ΔV/cm^3 mol^{-1}	ΔK/10^3 cm^3 mol^{-1} bar^{-1}
25	−59.2	15
50	−58.6	
75	−62.7	
100	−68.8	
125	−80.6	
150	−93.4	

The concentration and temperature dependence of the solubility product of the scaling minerals $CaCO_3$, $BaSO_4$, $SrSO_4$, $CaSO_4\cdot 2H_2O$ and $CaSO_4$ were obtained by fitting values of $K°_{sp}$ to simple temperature functions and then using model activity coefficients to calculate K_{sp} through eqn. (5),[2] where $\gamma_\pm$ is the mean ionic activity coefficient and

$$K_{sp} = K°_{sp}\,\gamma_\pm^{-2} = m_+^{\nu+}\,m_-^{\nu-} \qquad (5)$$

m_+, m_-, ν_+ and ν_- have their usual definitions. We used $K°_{sp}$ ($FeCO_3$) in the temperature region 25–200 °C, the solubility product of $FeCO_3$ at 25 °C obtained by Bardy and Péré[13] ($K_{sp} = 10^{-10.46}$), the data of Wagman *et al.*[14] and the data of Greenberg and Tomson[15] in the temperature region 25–94 °C to obtain the coefficients in eqn. (6), which are valid in the temperature region 25 °C–200 °C. We used the

$$pK°_{sp}(FeCO_3) = 21.804 + 0.02298\,(T/\mathrm{K})$$

$$-\,7.3134\log(T/\mathrm{K}) - 56.448\,(T/\mathrm{K})^{-1} \qquad (6)$$

program MODFIT,[16] which utilizes the simplex method, in our fitting procedure. A comparison between eqn. (6) and the $K°_{sp}$ data from which the model equation is based is shown in Fig. 1.

If the thermodynamic data of Barner and Scheuerman[17] were used to determine $K°_{sp}(FeCO_3)$ we obtained a value of $K°_{sp}$ which was only 1/3 of the values given elsewhere.[13–15,18,20]

Activity coefficients were obtained using the Pitzer model.[6–8] Those parameters which were not found in the literature for the multicomponent system H_2O–OH^-–H^+–CO_2–HCO_3^-–CO_3^{2-}–SO_4^{2-}–Cl^-–A^-–Na^+–K^+–Fe^{2+}–Mg^{2+}–Ca^{2+}–Sr^{2+}–Ba^{2+} were determined using solubility

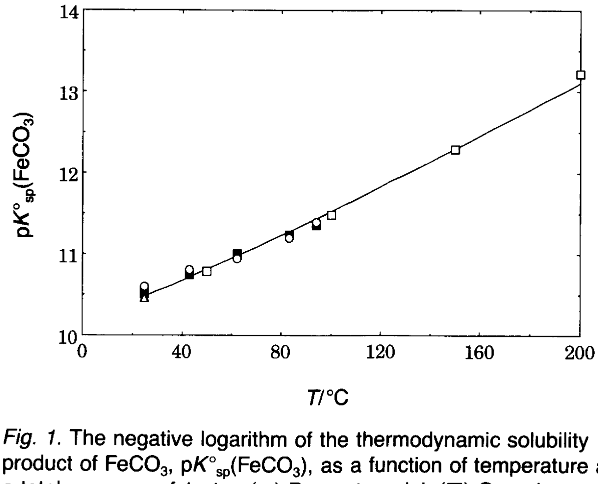

Fig. 1. The negative logarithm of the thermodynamic solubility product of $FeCO_3$, $pK°_{sp}(FeCO_3)$, as a function of temperature at a total pressure of 1 atm. (–) Present model, (■) Greenberg and Tomson,[15] (○) calculated from Wagman *et al.*[14] (see also Ref. 15), (□) Naumov *et al.*[20] and (△) Bardy and Péré.[13]

Table 2. The interaction parameters $\beta^{(0)}$, $\beta^{(1)}$ and $\beta^{(2)}$ for interactions between $Fe^{2+}(Ca^{2+})$ and four anions.

Ion pair	$\beta^{(0)}$	$\beta^{(1)}$	$\beta^{(2)}$	Ref.
Fe^{2+}–Cl^-	0.4479	2.043		8c
Fe^{2+}–HCO_3^-	0.0	14.76		This work
Fe^{2+}–CO_3^{2-}	1.919	−5.134	−274.0	This work
Fe^{2+}–SO_4^{2-} [a]	−4.705	17.00	−127.2	This work
Ca^{2+}–Cl^-	0.3053	1.708		4
Ca^{2+}–HCO_3^-	−1.498	7.899		4
Ca^{2+}–CO_3^{2-}	−0.400	−5.300	−879.2	4
Ca^{2+}–SO_4^{2-}	0.200	3.197	−54.24	4

[a]The β-parameters for Fe^{2+}–SO_4^{2-} interactions are determined using $FeCO_3$ solubilities. These parameters are somewhat arbitrary, since the value for $\beta^{(1)} = 17$ is equal to the limiting value allowed in the optimization procedure.

data. In a recent paper Bache *et al.*[4] determined both the parameters and the temperature derivatives of these parameters. Parameters for Fe^{2+} interactions were not included in their work.

For $FeCO_3$ solubility data are only available at 20 and 30°C. Based on these data and the available $K°_{sp}$ data, however, it is not possible to estimate reliable temperature derivatives of the Pitzer parameters for the Fe^{2+}–HCO_3^- and Fe^{2+}–CO_3^{2-} ion interactions. As mentioned earlier, $FeCO_3$ and $CaCO_3$ have some common properties in aqueous solutions at 25°C. We have therefore neglected the temperature derivatives for Fe^{2+}–CO_3^{2-} and Fe^{2+}–HCO_3^- interactions, as the equivalent temperature derivatives of the Ca interactions are zero.[4]

According to Pitzer[7] it is justified to neglect several of the parameters in the virial equation for the excess Gibbs

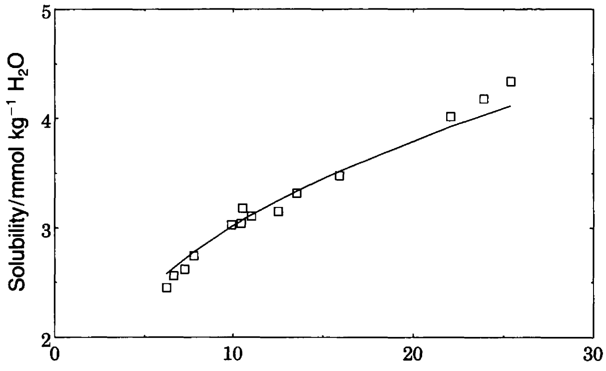

Fig. 2. Solubility of $FeCO_3$ in water at 30 °C at varying P_{CO_2}. (–) Model and (□) Smith.[18]

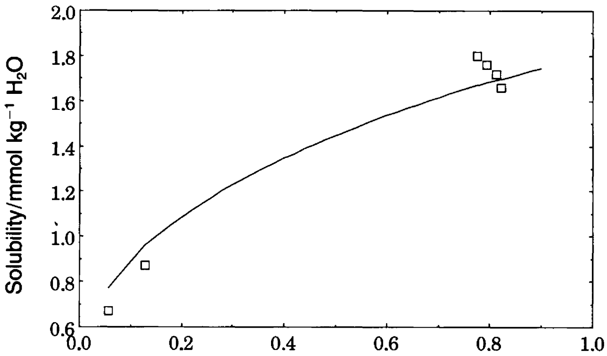

Fig. 3. Solubility of $FeCO_3$ in water at 20 °C at varying P_{CO_2}. (–) Model and (□) Bardy and Péré.[13]

Table 3. Model solubilities compared with experimental solubility data for $FeCO_3$ in different solutions.

System	T/°C	P_{CO_2}/atm	No. of exptl. data	Standard deviation (%)		Ref.
				β = 0	Optimal β-values	
$FeCO_3$ H_2O	20 30	0–1 5–25	6 14	10.1 13.1	8.3 2.9	13 18
$FeCO_3$ H_2O NaCl	20	0–1	5		5.4	13
$FeCO_3$ H_2O $MgCl_2$	20	0–1	5		2.1	13
$FeCO_3$ H_2O Na_2SO_4	20	0–1	5	9.4	2.9[a]	13
$FeCO_3$ H_2O $MgSO_4$	20	0–1	5	9.1	2.7[a]	13

[a]Not optimal values. See text and Table 2.

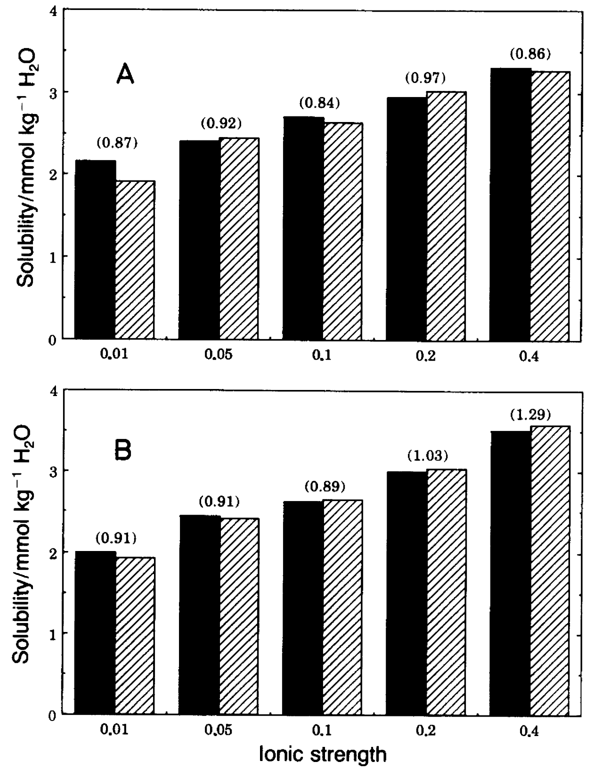

Fig. 4. Solubility of $FeCO_3$ in NaCl (A) and $MgCl_2$ (B) solutions at 20 °C at varying ionic strength and P_{CO_2}, which is given over each column. (■) Model and (▨) Bardy and Péré.[13]

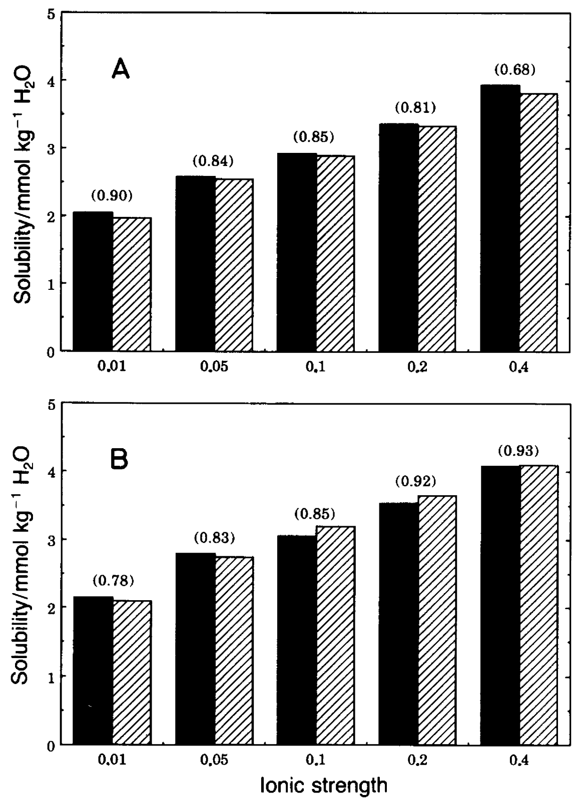

Fig. 5. Solubility of $FeCO_3$ in Na_2SO_4 (A) and $MgSO_4$ (B) solutions at 20 °C at varying ionic strength and P_{CO_2}, which is given over each column. (■) Model and (▨) Bardy and Péré.[13]

energy of the system when the ionic strength of the solution is less than 2 M. Waters produced during oil recovery normally have an ionic strength ≤ 1.0 M. For $FeCO_3$ in such waters we may therefore use a simplified Pitzer activity coefficient equation.[8a] This equation is given in Appendix 1.

In Table 2 the β-interaction parameters determined in the present work for some Fe^{2+}–X^{n-} interactions are given, together with the corresponding Ca^{2+} interactions.[4] The values given for the Fe^{2+}–SO_4^{2-} interaction are uncertain, since these parameters are determined indirectly via the $FeCO_3$ solubility data in Na_2SO_4 and $MgSO_4$ solutions. The high value of $\beta^{(1)}$ also incates that these parameters are not true representations of Fe^{2+}–SO_4^{2-} interactions. As can be observed from Table 3, however, there is a reasonable agreement between experimental solubilities of $FeCO_3$ and model predictions when the optimal β-parameters in Table 2 are used.

In Figs. 2 and 3 the data of Smith[18] and of Bardy and Péré[13] are compared with model data for $FeCO_3$ solubilities in H_2O at varying P_{CO_2} at 30 and 20 °C, respectively.

In Figs. 4 and 5 the model solubilities at varying ionic strength are compared with the data of Bardy and Péré[13] It should be noted, however, that some of the data of Bardy and Péré have been used to obtain the β-parameters for the Fe^{2+}–SO_4^{2-} interactions. The experimental data and model predictions shown in Figs. 2, 3 and 5 are therefore not independent.

The equilibrium model

When the ions Fe^{2+}, Ca^{2+}, Sr^{2+}, Ba^{2+}, CO_3^{2-} and SO_4^{2-}, together with an organic acid, HA, are present in a sea-water type of solution in equilibrium with an oil and a gas phase containing CO_2, it is necessary to establish a set of equations describing the precipitation equilibria in order to be able to calculate the amounts of the different minerals which may precipitate.

Possible equilibria.

$$FeCO_3(s) = Fe^{2+} + CO_3^{2-} \quad K_{sp}(FeCO_3) \quad (7)$$

$$CaCO_3(s) = Ca^{2+} + CO_3^{2-} \quad K_{sp}(CaCO_3) \quad (8)$$

$$CaSO_4(s) = Ca^{2+} + SO_4^{2-} \quad K_{sp}(CaSO_4) \quad (9)$$

$$CaSO_4 \cdot 2H_2O(s) = Ca^{2+} + SO_4^{2-} + 2H_2O \quad K_{sp}(CaSO_4 \cdot 2H_2O) \quad (10)$$

$$SrSO_4(s) = Sr^{2+} + SO_4^{2-} \quad K_{sp}(SrSO_4) \quad (11)$$

$$BaSO_4(s) = Ba^{2+} + SO_4^{2-} \quad K_{sp}(BaSO_4) \quad (12)$$

$$CO_2(g) = CO_2(aq) \qquad K_H(CO_2) \qquad (13)$$

$$CO_2(aq) = CO_2(oil) \qquad K_O(CO_2) \qquad (14)$$

$$CO_2(aq) + H_2O = HCO_3^- + H^+ \qquad K_1(H_2CO_3) \qquad (15)$$

$$HCO_3^- = CO_3^{2-} + H^+ \qquad K_2(H_2CO_3) \qquad (16)$$

$$HA = A^- + H^+ \qquad K_{HA} \qquad (17)$$

$$H_2O = H^+ + OH^- \qquad K_w \qquad (18)$$

HA is the symbol for a general organic acid.

Mass balances.

$$m^o_{Fe^{2+}} = m_{FeCO_3(s)} + m_{Fe^{2+}} \qquad (19)$$

$$m^o_{Ca^{2+}} = m_{CaCO_3(s)} + m_{CaSO_4(s)} + m_{CaSO_4\cdot 2H_2O(s)} + m_{Ca^{2+}} \qquad (20)$$

$$m^o_{Sr^{2+}} = m_{SrSO_4(s)} + m_{Sr^{2+}} \qquad (21)$$

$$m^o_{Ba^{2+}} = m_{BaSO_4(s)} + m_{Ba^{2+}} \qquad (22)$$

$$m^o_{SO_4^{2-}} = m_{CaSO_4(s)} + m_{CaSO_4\cdot 2H_2O(s)} + m_{SrSO_4(s)} + m_{BaSO_4(s)} + m_{SO_4^{2-}} \qquad (23)$$

$$m^o_{HA} = m_{A^-} + m_{HA} \qquad (24)$$

$$m^o_{CO_2} = m_{CO_2(g)} + m_{CO_2(o)} + m_{CO_2(aq)} + m_{CaCO_3(s)} + m_{FeCO_3(s)} \qquad (25)$$

In these equations m_i is the molal concentration of component i, and o indicates the oil phase.

Electroneutrality. In the electroneutrality equation we will only consider those ions which may precipitate or which may change composition owing to the precipitation reactions. The sum of the positive charges minus the negative ones will thus be a constant, given by eqn. (26).

$$k = 2m_{Fe^{2+}} + 2m_{Ca^{2+}} + 2m_{Sr^{2+}} + 2m_{Ba^{2+}} + m_{H^+} - 2m_{SO_4^{2-}} - 2m_{CO_3^{2-}} - m_{HCO_3^-} - m_{A^-} - m_{OH^-} \qquad (26)$$

Model calculation. In our calculation we consider only precipitation of either anhydrite, $CaSO_4$, or gypsum, $CaSO_4\cdot 2H_2O$. We therefore have 19 unknowns and 19 equations. These equations can be combined into two equations with two unknowns. These equations, eqns. (27) and (28), with the concentrations of HCO_3^- and H^+ as the unknowns, are given below.

$$2C_3m_{H^+}/m_{HCO_3^-} - 2C_4m_{HCO_3^-}/m_{H^+} + m_{H^+} - m_{HCO_3^-} - K_w/m_{H^+} - C_5/(K_{HA} - m_{H^+}) - k = 0 \qquad (27)$$

$$C_8m_{H^+}m_{HCO_3^-} - C_3m_{H^+}/m_{HCO_3^-} + C_4m_{HCO_3^-}/m_{H^+} + m_{HCO_3^-} + C_7 = 0 \qquad (28)$$

In Appendix 2 the coefficients in eqns. (27) and (28) are given. The reason for choosing HCO_3^- and H^+ as unknowns is given by the fact that first estimates of these concentrations are relatively easy to guess for formation waters. Using a Newton–Raphson iteration method in two dimensions,[21] the equations are solved numerically. The solution gives the ionic composition in the aqueous phase and the amount of the different minerals precipitated after equilibrium is established. Both dissolution and precipitation reactions are considered.

In the present algorithm we have taken proper consideration of the fact that the various scale components of a mixed scale do not precipitate sequentially but more or less simultaneously, particularly at high degrees of supersaturation. Minerals which are "precipitated" in the early stages of the calculation are "dissolved" if the apparent solubility product, m_+m_-, becomes less than the true K_{sp}.[12]

We will now give some examples of how our equilibrium model, together with our solubility models for the precipitating minerals, can be used to estimate the effect of Fe^{2+} concentration on carbonate scaling.

Precipitation of $FeCO_3$ and $CaCO_3$ from formation waters

The effect of Fe^{2+} concentration. The precipitation of carbonates will normally occur in the production tubing and equipment owing to CO_2 degasing. At high pressures (above the bubble point of the oil–water system) the CO_2 content of the liquids will be high, the pH will be low, and

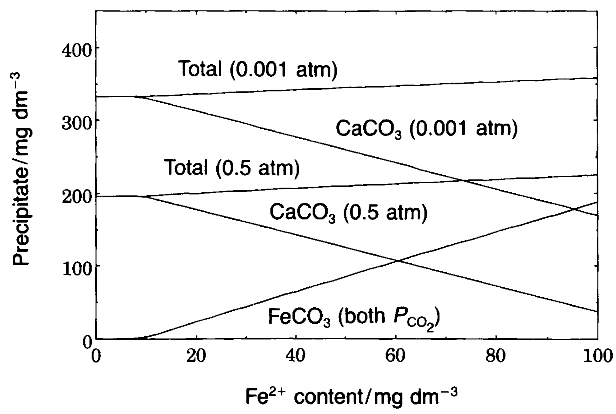

Fig. 6. The influence of Fe^{2+} concentration on carbonate precipitation in the formation water given in Table 4. T = 100 °C, $C_{Ca^{2+}}$ = 1275 mg dm^{-3} and P_{CO_2} = 0.001 and 0.5 atm, respectively.

Table 4. Water analysis at 20 °C, P_{tot} = 1 bar and P_{CO_2} = 0.

Ion	Formation water/mg dm^{-3} (pH 5.5)	Sea water/mg dm^{-3} (pH 7.95)
Na^+	14 834	12 465
K^+	0	0
Mg^{2+}	335	1 130
Ca^{2+}	1 275	450
Sr^{2+}	335	9
Ba^{2+}	50	0
Fe^{2+}	30	0
Cl^-	26 200	20 950
SO_4^{2-}	0	3 077
HCO_3^-	415	170

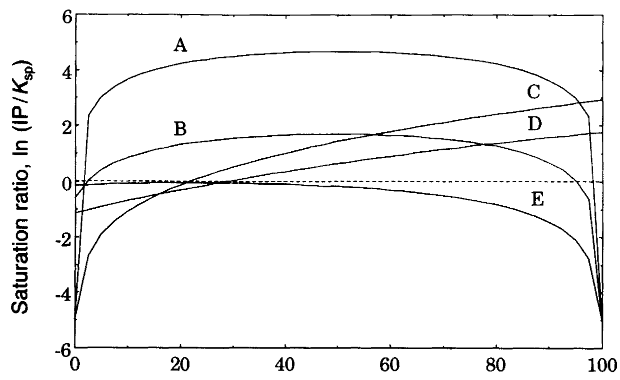

Fig. 7. Saturation ratio, ln (IP/K_{sp}) where IP = m_+ m_-, as a function of formation water content in mixed waters made up from the two waters given in Table 4 at T = 100 °C, P_{CO_2} = 0.5 atm and P_{tot} = 1 atm. (A) $BaSO_4$, (B) $SrSO_4$, (C) $FeCO_3$, (D) $CaCO_3$ and (E) $CaSO_4$.

as a consequence low CO_3^{2-} concentrations will appear in the aqueous phase.

Since the kinetics of $FeCO_3$ precipitation is not included in the present model, we will only discuss equilibrium consequences of introducing Fe^{2+} into the waters. We will thus not try to calculate the amount of scale precipitating in certain areas of the production system, since such calculations are very dependent on the rates of the precipitating reactions.[3] Since siderite precipitation is several orders of magnitude slower than calcite precipitation at ground water and water treatment temperatures,[15] siderite scaling will be considerably delayed relative to calcite scaling in production tubings and may not be precipitated at all. In Fig. 6 the influence of Fe^{2+} on the carbonate precipitation at 100 °C and P_{CO_2} = 0.001 atm (0.500 atm) at constant concentration of Ca^{2+} in the water is given. Apart from the Fe^{2+} and Cl^- concentrations the ion concentrations in the waters are the same as those given for the formation water in Table 4. At a certain Fe^+ content, $C_{Fe^{2+}} \approx 10$ mg dm^{-3}, $FeCO_3$ starts to precipitate. As the Fe^{2+} content increases, $FeCO_3$ precipitation increases and $CaCO_3$ precipitation decreases, as expected. The total carbonate precipitation (in mg dm^{-3}) increases slightly from $C_{Fe^{2+}} = 0$ to $C_{Fe^{2+}} = 100$ mg dm^{-3}. Since K_{sp} ($FeCO_3$) < K_{sp} ($CaCO_3$), however, there is a slight increase in the number of moles of precipitate. For all practical purposes we may assume a carbonate precipitation which is independent of Fe^{2+} concentration. When P_{CO_2} increases, the total carbonate precipitation is decreased by the same amount as observed for the $CaCO_3$–H_2O system ($C_{Fe^{2+}} = 0$).

Figs. 7 and 8 show the initial saturation ratio ln (m_+m_-/K_{sp}) and the amount of precipitate formed of the different scale-forming minerals when the two waters in Table 4 are mixed. Even if the saturation ratios of $BaSO_4$ and $FeCO_3$ are larger than for the other minerals for most concentrations, the amounts of precipitate formed from these minerals are relatively small owing to the combina-

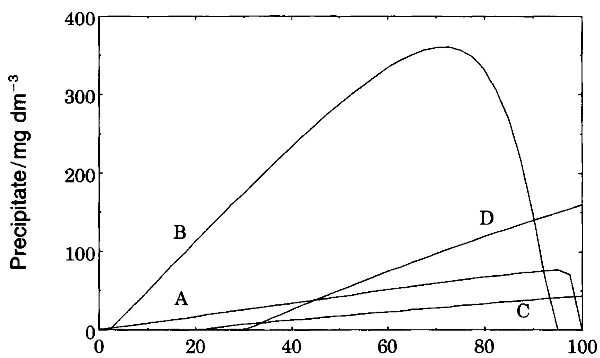

Fig. 8. Mineral precipitate as a function of formation water content in mixed waters made up from the two waters given in Table 4 at T = 100 °C, P_{CO_2} = 0.5 and P_{tot} = 1 atm. (A) $BaSO_4$, (B) $SrSO_4$ (C) $FeCO_3$ and (D) $CaCO_3$.

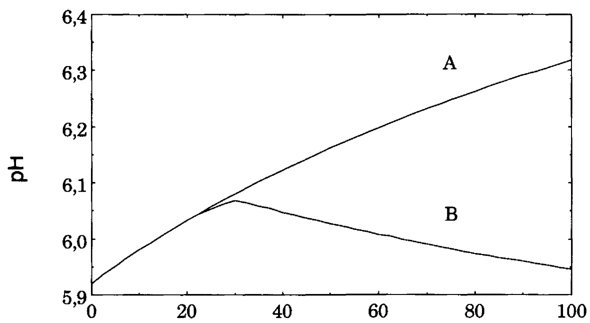

Fig. 9. pH as a function of formation water content in mixed waters made up from the two waters given in Table 4 at T = 100 °C, P_{CO_2} = 0.5 atm and P_{tot} = 1 atm. (A) pH in initial waters before carbonate precipitation. (B) pH at equilibrium. The effect of reaching $CaCO_3$ saturation at ≈ 30 vol % formation water and $FeCO_3$ saturation at ≈ 23 vol % formation water is observed.

tion of the low solubility products and the low concentrations of Ba^{2+} and Fe^{2+} in the waters. In Fig. 9 the pH variation with the fraction of formation water in mixed waters corresponding to those shown in Figs. 7 and 8 is given. The effect of both $CaCO_3$ and $FeCO_3$ precipitation on the pH can be observed.

The effect of an organic acid. The species in the carbonate system are not analysed separately; the invidual concentrations are found from measuring the total alkalinity, A_T, together with either the pH or P_{CO_2}. The total alkalinity is

$$A_T = m_{HCO_3^-} + 2m_{CO_3^{2-}} + m_{A^-} + m_{OH^-} - m_{H^+} \quad (29)$$

defined by eqn. (29). A common assumption when determining the distribution of the species in the carbonate system is to set A_T equal to the carbonate alkalinity, A_C

$$A_T \approx A_C = m_{HCO_3^-} + 2m_{CO_3^{2-}} \quad (30)$$

[eqn. (30)]. This assumption, however, may cause serious errors if an organic acid (or another weak acid), is present in the water. As reported by Barth,[22] the amount of organic acids from North Sea oil reservoirs does in some instances exceed 1000 mg dm^{-3}. In Fig. 10 predicted $CaCO_3$ and $FeCO_3$ precipitation from a typical North Sea formation water (Table 4) is plotted versus the content of organic acid at constant total alkalinity.

The water analysis used in the calculations presented in Fig. 10 is given in Table 4. Fig. 10 illustrates how the predicted precipitation of $CaCO_3$ steadily decreases when an organic acid (such as acetic acid) is introduced into the water. $CaCO_3$ is dissolved to a much higher degree than $FeCO_3$ at small additions of organic acid, and there is no noticeable dissolution of $FeCO_3$ until all $CaCO_3$ is dissolved. This effect is due to the much higher solubility of $CaCO_3$ than $FeCO_3$.

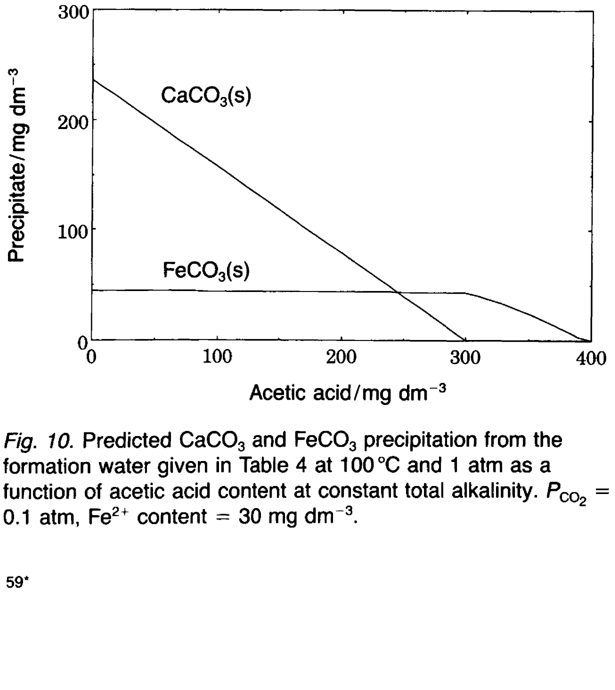

Fig. 10. Predicted $CaCO_3$ and $FeCO_3$ precipitation from the formation water given in Table 4 at 100 °C and 1 atm as a function of acetic acid content at constant total alkalinity. P_{CO_2} = 0.1 atm, Fe^{2+} content = 30 mg dm^{-3}.

Concluding remarks. At low Fe^{2+} levels (< 10 ppm) $FeCO_3$ scaling should not be a problem in formation waters of normal calcium concentrations. In acid wells, however, Fe^{2+} may easily increase and $FeCO_3$ precipitation may lead to scaling. If Ca^{2+} is present, this will result in a reduction in $CaCO_3$ precipitation and no increase in the total carbonate precipitation will occur.

In wells containing acids in addition to H_2CO_3 it is important to obtain reliable data on the concentration of these acids in the produced waters if $CaCO_3$ scaling is to be estimated.

Possible FeS scaling and other forms of iron precipitation, such as the formation of oxides or hydroxides, however, may also give operational problems. In a forthcoming paper the problems arising due to the presence of hydrogen sulfide will be addressed.

Appendix 1

The $FeCO_3$ activity coefficient, γ_{FeCO_3}, in aqueous electrolytes according to Pitzer.[8a] *Ionic strength* < 2 M.

Ionic species: H_2O–OH^-–H^+–CO_2–HCO_3^-–CO_3^{2-}–SO_4^{2-}–Cl^-–A^-–Na^+–K^+–Fe^{2+}–Mg^{2+}–Ca^{2+}–Sr^{2+}–Ba^{2+}.

$$\ln\gamma_{FeCO_3} = 4f' + m_{OH^-}B_{Fe-OH} + m_{Cl^-}B_{Fe-Cl} + m_{SO_4^{2-}}B_{Fe-SO_4} +$$

$$m_{HCO_3^-}B_{Fe-HCO_3} + m_{CO_3^{2-}}B_{Fe-CO_3} + m_{A^-}B_{Fe-A} +$$

$$m_{H^+}B_{H-CO_3} + m_{Na^+}B_{Na-CO_3} + m_{K^+}B_{K-CO_3} + m_{Mg^{2}}B_{Mg-CO_3} +$$

$$m_{Ca^{2+}}B_{Ca-CO_3} + m_{Sr^{2+}}B_{Sr-CO_3} + m_{Ba^{2+}}B_{Ba-CO_3} + m_{Fe^{2+}}B_{Fe-CO_3} +$$

$$4m_{H^+}(m_{OH^-}B'_{H-OH} + m_{Cl^-}B'_{H-Cl} + m_{SO_4^{2-}}B'_{H-SO_4} +$$

$$m_{HCO_3^-}B'_{H-HCO_3} + m_{CO_3^{2-}}B'_{H-CO_3} + m_{A^-}B'_{H-A}) +$$

$$4m_{Na^+}(m_{OH^-}B'_{Na-OH} + m_{Cl^-}B'_{Na-Cl} + m_{SO_4^{2}}B'_{Na-SO_4} +$$

$$m_{HCO_3^-}B'_{Na-HCO_3} + m_{CO_3^{2-}}B'_{Na-CO_3} + m_{A^-}B'_{Na-A}) +$$

$$4m_{K^+}(m_{OH^-}B'_{K-OH} + m_{Cl^-}B'_{K-Cl} + m_{SO_4^{2-}}B'_{K-SO_4} +$$

$$m_{HCO_3^-}B'_{K-HCO_3} + m_{CO_3^{2-}}B'_{K-CO_3} + m_{A^-}B'_{K-A}) +$$

$$4m_{Mg^{2+}}(m_{OH^-}B'_{Mg-OH} + m_{Cl^-}B'_{Mg-Cl} + m_{SO_4^{2-}}B'_{Mg-SO_4} +$$

$$m_{HCO_3^-}B'_{Mg-HCO_3} + m_{CO_3^{2-}}B'_{Mg-CO_3} + m_{A^-}B'_{Mg-A}) +$$

$$4m_{Ca^{2+}}(m_{OH^-}B'_{Ca-OH} + m_{Cl^-}B'_{Ca-Cl} + m_{SO_4^{2-}}B'_{Ca-SO_4} +$$

$$m_{HCO_3^-}B'_{Ca-HCO_3} + m_{CO_3^{2-}}B'_{Ca-CO_3} + m_{A^-}B'_{Ca-A}) +$$

$$4m_{Sr^{2+}}(m_{OH^-}B'_{Sr-OH} + m_{Cl^-}B'_{Sr-Cl} + m_{SO_4^{2-}}B'_{Sr-SO_4} +$$

$$m_{HCO_3^-}B'_{Sr-HCO_3} + m_{CO_3^{2-}}B'_{Sr-CO_3} + m_{A^-}B'_{Sr-A}) +$$

$$4m_{Ba^{2+}}(m_{OH^-}B'_{Ba\text{-}OH} + m_{Cl^-}B'_{Ba\text{-}Cl} + m_{SO_4^{2-}}B'_{Ba\text{-}SO_4} + m_{HCO_3^-}B'_{Ba\text{-}HCO_3} + m_{CO_3^{2-}}B'_{Ba\text{-}CO_3} + m_{A^-}B'_{Ba\text{-}A}) + 4m_{Fe^{2+}}(m_{OH^-}B'_{Fe\text{-}OH} + m_{Cl^-}B'_{Fe\text{-}Cl} + m_{SO_4^{2-}}B'_{Fe\text{-}SO_4} + m_{HCO_3^-}B'_{Fe\text{-}HCO_3} + m_{CO_3^{2-}}B'_{Fe\text{-}CO_3} + m_{A^-}B'_{Fe\text{-}A}) \quad (A.1)$$

where

$$B = \beta^{(0)} + \frac{2\beta^{(1)}}{\alpha_1^2 I}[1 - (1 + \alpha_1 I^{1/2})\exp(-\alpha_1 I^{1/2})] + \frac{2\beta^{(2)}}{\alpha_2^2 I}[1 - (1 + \alpha_2 I^{1/2})\exp(-\alpha_2 I^{1/2})] \quad (A.2)$$

and

$$B' = d\beta/dI$$

In this equation m_i denotes the molality of ion i, α_1 and α_2 are constants equal to 1.4 $kg^{1/2}\ mol^{-1/2}$ and 12 $kg^{1/2}\ mol^{-1/2}$, respectively, for interactions between divalent ions, while $\alpha_1 = 2\ kg^{1/2}\ mol^{-1/2}$ and $\alpha_2 = 0$ for interactions between univalent and divalent and between two univalent ions. I is the ionic strength and $4f^{\gamma}$ the extended Debye–Hückel contribution to ln γ.[8b] The $\beta^{(0)}$, $\beta^{(1)}$ and $\beta^{(2)}$ parameters are due to short-range coulombic interactions between two ions. These constants are independent of composition and may, when determined, be used in any mixed electrolyte system where these two ions occur. $\beta^{(2)} = 0$ for interactions between two ions where at least one is univalent.

Appendix 2

Constants C_1–C_8 in eqns. (27) and (28).

$$C_1 = \frac{K_{sp}(CaCO_3)}{K_2(H_2CO_3)} \quad (A.3)$$

If $CaCO_3$ precipitates, but not $CaSO_4$:

$$C_2 = 0. \quad (A.4)$$

If both $CaCO_3$ and $CaSO_4$ precipitate:

$$C_2 = \frac{C_1}{K_{sp}(CaSO_4)} \quad (A.5)$$

$$C_3 = C_1 + C_2\left(K_{sp}(BaSO_4) + K_{sp}(SrSO_4) + \frac{K_{sp}(FeCO_3)}{K_2(H_2CO_3)}\right) \quad (A.6)$$

In eqn. (A.5), $K_{sp}(BaSO_4)$ [$K_{sp}(SrSO_4)$] is greater than zero only when $BaSO_4$ ($SrSO_4$) precipitates simultaneously with both $CaCO_3$ and $CaSO_4$. $K_{sp}(FeCO_3)$ is equal to zero when $FeCO_3$ does not precipitate.

If $CaCO_3$ precipitates, but not $CaSO_4$:

$$C_4 = K_2(H_2CO_3) \quad (A.7)$$

If both $CaCO_3$ and $CaSO_4$ precipitate:

$$C_4 = K_2(H_2CO_3) + \frac{1}{C_2} \quad (A.8)$$

$$C_5 = m^{\circ}_{HA}K_{HA} \quad (A.9)$$

$$C_6 = \frac{V}{Z\,R\,T\,W_{H_2O}} \quad (A.10)$$

If $CaCO_3$ or $FeCO_3$ precipitate, $CaSO_4$ does not precipitate simultaneously with $CaCO_3$.

$$C_7 = m^{\circ}_{Ca^{2+}} + m^{\circ}_{Fe^{2+}} - m^{\circ}_{CO_2} \quad (A.11)$$

If MCO_3 does not precipitate, $m^{\circ}_M = 0$.

If both $CaCO_3$ and $CaSO_4$ precipitate:

$$C_7 = m^{\circ}_{Ca^{2+}} + m^{\circ}_{Ba^{2+}} + m^{\circ}_{Sr^{2+}} + m^{\circ}_{Fe^{2+}} + m^{\circ}_{SO_4^{2-}} + m^{\circ}_{CO_2} \quad (A.12)$$

In eqn. (A.12) $m^{\circ}_{Ba^{2+}}$ is greater than zero when $BaSO_4$ precipitates, otherwise zero. The same procedure applies for $SrSO_4$ and $FeCO_3$.

$$C_8 = \frac{C_6}{K_H K_1(H_2CO_3)} + \frac{K_0\,W_{oil}}{W_{H_2O}K_1(H_2CO_3)} + \frac{1}{K_1(H_2CO_3)} \quad (A.13)$$

In these equations V_{gas} is the gas volume in m^3, W_{oil} is the mass of oil in kg and W_{H_2O} is the mass of water in kg.

References

1. Haarberg, T., Seim, I., Skjørholm, S. J., Østvold, T., Read, P. and Schmidt, T. In: Ogden, P. H., Ed., *Third International Symposium on Chemicals in the Oil Industry,* Manchester, April 1988. Royal Society of Chemistry, London 1988, p. 121.
2. Haarberg, T., Granbakken, D. B., Seim, I., Østvold, T., Read, P. and Schmidt, T. *To be published.*
3. Granbakken, D. B., Haarberg, T., Rollheim, M., Østvold, T., Read, P. and Schmidt, T. *To be published.*
4. Bache, Ø., Haarberg, T. and Østvold, T. *To be published.*
5. Abrams, D. S. and Prausnitz, J. M. *AIChE J. 21* (1975) 116.
6. Pitzer, K. S. *J. Phys. Chem. 77* (1973) 268.
7. Pitzer, K. S. *Pure Appl. Chem. 58* (1986) 1599.

8. Pitzer, K. S. In: Pytkowicz, R. M., Ed., *Activity Coefficients in Electrolyte Solutions,* CRS Press, Boca Raton, Fl 1977; (a) p. 172; (b) p. 170, eqn. (47); (c) p. 183.
9. Cowan, J. C. and Weintritt, D. J. *Water-Formed Scale Deposits,* Gulf Publishing Co., Houston, TX 1976, p. 186.
10. Weast, R. C. *Handbook of Chemistry and Physics,* 50th ed., CRC Press, Cleveland, OH 1969–1970.
11. Millero, F. J. *Geochim. Cosmochim. Acta 46* (1982) 11.
12. Haarberg, T. *Thesis,* Institute of Inorganic Chemistry, NTH, University of Trondheim, Trondheim, Norway 1989.
13. Bardy, J. and Péré, C. *Trib. Cebedean 29* (1976) 75.
14. Wagman, D. D., Evans, W. H., Parker, V. B., Schumm, R. H., Halow, I., Bailey, S. M., Churney, K. L. and Nutall, L. *J. Phys. Chem. Ref. Data II (Suppl. 2)* (1982).
15. Greenberg, J. and Tomson, M. *Am. J. Sci. Submitted.*
16. Hertzberg, T. *MODFIT:* Institute of Chemical Engineering, NTH, University of Trondheim, Trondheim, Norway 1982.
17. Barner, H. E. and Scheuerman, R. V. *Handbook of Thermo-Chemical Data for Compounds and Aqueous Species,* Wiley, New York, NY 1982.
18. Smith, H. *J. Am. Chem. Soc. 40* (1918) 879.
19. Singer, Ph. C. and Stumm, W. *JAWW Assoc. 62* (1970) 198.
20. Naumov, G. B., Ryzhenko, B. N. and Khodakovsky, I. L. *Handbook of Thermodynamic Data,* U.S. Geological Survey Water Resources Division, Menlo Park, CA 1974.
21. Johnson, L. W. and Riess, R. D. *Numerical Analysis,* Addison-Wesley, Reading, MA 1982, p. 169.
22. Barth, T. *Internal Report,* University of Bergen, Bergen 1989.

Received April 6, 1990.